Gauss Modes in Cylindrical Cavities

Franziska Nieder, Maik Holzhey and Lauri Schwenson

***Abstract*—Gauss Modes are of particularly high interest as field solutions in cylindrical cavities, when engineering resonators, suitable for laser applications. Therefore, an analytical study and comprehensive numerical calculations are provided to obtain accurate field solutions. Numeric calculations, using the Finite-Integration-Technique, give solutions for eigenmodes and transient fields. Formulas to calculate field solutions analytically and numerically are provided in this paper. Furthermore, different numeric implementations are compared and evaluated.**

I. Introduction

Performing numeric calculations of optical field solutions with sufficient accuracy remains a challenge even for modern day computers. Long calculation times, up to several days on an office workstation for standard optical applications, are unsuitable to do R&D tasks efficiently. However, due to symmetry in some geometries the numeric modelling can be of significantly less complexity while remaining full accuracy. Cylindrical structures can be reduced to a single 2D rz plane which is finally used to reconstruct the azimuthal dependency. Commercial software, like CST *Microwave Studio* [1], does not support such a feature. This paper presents an easy to implement numeric algorithm to make use of such a powerful symmetry condition. We provide solutions for Gauss eigenmodes in cylindrical cavities with a curved mirror as well as a time-domain solution to simulate transient electromagnetic fields. Finally, the benefits over a standard commercial software are analysed. | MH·FN·LS |

II. Theory

The optical cavity in this paper consists of a plane and a curved mirror facet. The curved mirror facet implies a curved phase front of the oscillating field. Herewith, the Gaussian beam solution offers the possibility to calculate an analytic field distribution for an oscillating field between two opposite mirrors [2]. Firstly, the wave equation, assuming x-polarised light, is simplified to a scalar representation:

$$\Delta E_x + k^2 E_x = 0 \quad , \quad E_x = U(x,y,z) \cdot e^{-jkz} \tag{1}$$

$U(x,y,z)$ is the scalar amplitude of the field. This gives equation (2). which can be transformed to cylindrical coordinates to fit the problem geometry.

$$\frac{\partial^2 U}{\partial x^2} + \frac{\partial^2 U}{\partial y^2} + \frac{\partial^2 U}{\partial z^2} - 2jk\frac{\partial U}{\partial z} = 0 \tag{2}$$

It is now easy to see that the azimuthal dependency can be separated and the remaining function $u(r,z)$ can be solved by the following equations (3)-(6) [2].

$$u(r,z) = \frac{w_0}{w} \cdot \exp\left[-j(kz - \Phi) - r^2\left(\frac{1}{w^2} + j\frac{k}{2R}\right)\right] \tag{3}$$

This work was supported by Technische Universität Berlin (Berlin Institute of Technology), Faculty of Electrical Engineering and Computer Science, Department Theoretical Electromagnetics

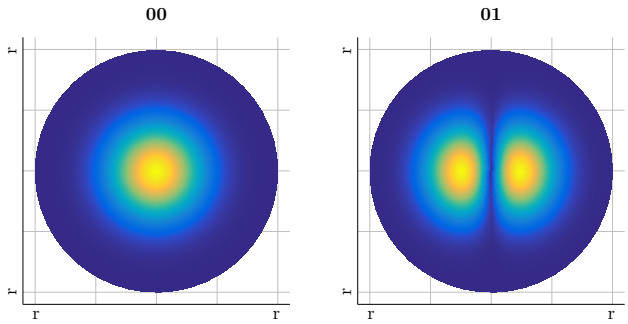

Fig. 1. Absolute magnitude field distribution of transversal Gauss modes of radial *p* and azimuthal *l* mode order: *pl*. The near zero field values (deep blue) at boundary are a characteristic feature of Gauss modes.

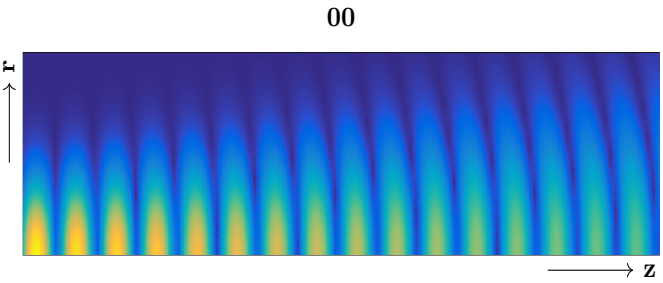

Fig. 2. Absolute magnitude field distribution of a Gaussian beam field in rz plane of *pl* 00 mode

Equation (3) gives the Gaussian field distribution in rz plane (compare fig. 2). The radius of curvature R of the propagating phase front is defined as:

$$R(z) = z\left[1 + \left(\frac{\pi w_0^2}{\lambda z}\right)^2\right] \tag{4}$$

While λ is the wavelength, equation (5) gives the spot size radius w of the Gaussian field depending on the evaluated fields position z in reference to an initial spot size radius w_0.

$$w^2(z) = w_0^2 \cdot \left[1 + \left(\frac{\lambda z}{\pi w_0^2}\right)^2\right] \tag{5}$$

The remaining formulas, given in (6), provide the wave number k and the mode dependent phase information to equation (3). While p is the radial mode number and l refers to the azimuthal mode number.

$$k = \frac{2\pi}{\lambda} \quad , \quad \Phi = (2p + l + 1) \cdot \operatorname{atan}\left(\frac{\lambda z}{\pi w_0^2}\right) \tag{6}$$

Using the solution of the separated ordinary differential equation for φ and multiplying it with $u(r,z)$ gives the full 3D field solution (compare fig. 1).

$$\begin{aligned} U(r,z,\varphi) &= u(r,z) \cdot e^{-jl\varphi} \\ \vec{U}(r,z,\varphi) &= \vec{u}(r,z) \cdot \vec{f}(\varphi) \end{aligned} \tag{7}$$

The wave equation (1) was simplified to a scalar equation. However, solving Maxwell equations numerically will take vectorial information into account. The x-polarised light (1) needs to hold up when extending the field to its full azimuthal representation. The function extending $\vec{u}(r,z)$ needs to be modified for each vectorial component (8) [3]. The azimuthal mode number is $m = 1$ (compare fig. 3).

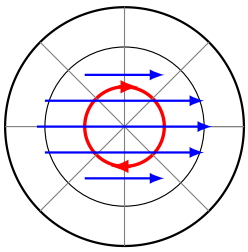

Fig. 3. Azimuthal mode order $m = 1$ *(blue)*

$$\begin{array}{ll} H_r(r,\varphi,z) \propto sin(m\varphi) & E_r(r,\varphi,z) \propto cos(m\varphi) \\ H_\varphi(r,\varphi,z) \propto cos(m\varphi) & E_\varphi(r,\varphi,z) \propto sin(m\varphi) \\ H_z(r,\varphi,z) \propto sin(m\varphi) & E_z(r,\varphi,z) \propto cos(m\varphi) \end{array} \tag{8}$$

The **F**inite-**I**ntegration-**T**echnique (FIT) [4] can now be applied to solve this problem numerically. Making use of the azimuthal symmetry is crucial to obtain an advantage in calculation time over commercial software. However, Maxwell equations are innately defined as 3D. Therefore the rz grid is extended by virtual φ edges (compare: ***B**ody **o**f **R**evolution* (BOR) [5]). All elementary FIT linear operators $P_{r,\varphi,z}|_{m=1}$ need to be generated for the appropriate azimuthal mode order $m = 1$.

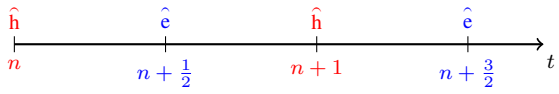

$$\begin{aligned} \hat{\mathrm{h}}^{(n+1)} &= \hat{\mathrm{h}}^{(n)} - \Delta t\; M_\mu^{-1} C\; \hat{\mathrm{e}}^{(n+\frac{1}{2})} \\ \hat{\mathrm{e}}^{(n+\frac{3}{2})} &= \hat{\mathrm{e}}^{(n+\frac{1}{2})} + \Delta t\; M_\varepsilon^{-1} \tilde{C}\; \hat{\mathrm{h}}^{(n+1)} \end{aligned} \tag{9}$$

Equation (9) allows to compute transient fields inside the cavity, using an explicit time-stepping scheme [6]. Ensuring numeric stability a maximum time step Δt_{max} must not be exceeded. A possible criterion to calculate a stable time step is given by (10). Besides the discrete electromagnetic energy should be monitored to remain within bound [5].

$$A_{cc}^{(E)} = M_\varepsilon^{-1} \tilde{C} M_\mu^{-1} C \quad , \quad \Delta t_{max} = 2 \cdot \left(\lambda_{eig|max}^{A} \right)^{-\frac{1}{2}} \tag{10}$$

A **t**ime-**d**omain (TD) calculation can lead to very long simulation times if a settled field condition needs to be analysed. Eigenmodes offer a quicker calculation method as they represent such a state. Using Matlab [7], those can easily be calculated by `eigs()` and the system matrix:

$$A_{curlcurl}^{(D)} = L_{32} \tilde{C} M_\mu^{-1} C M_\varepsilon^{-1} L_{23} \tag{11}$$

Using the divergence law $\tilde{S}\hat{\hat{\mathrm{d}}} = 0$ to avoid static modes, the matrices L_{23}, L_{32} can be derived [8].

$$L_{23} = \begin{bmatrix} I & 0 \\ -\frac{1}{m}\tilde{P}_r & -\frac{1}{m}\tilde{P}_z \\ 0 & I \end{bmatrix} \quad , \quad L_{32} = \begin{bmatrix} I & 0 & 0 \\ 0 & 0 & I \end{bmatrix} \tag{12}$$

Finally, to satisfy the desired azimuthal mode order, components of the electric field allocated directly at the z-axis need to be zeroed, as they cannot exit due to the cylindrical geometry and $m = 1$ (compare fig. 3). The latter modification needs to be applied to time-domain and eigenmode expansion, respectively. | MH |

III. Numerical Evaluation

A. Model

The plane mirror is defined by a **P**erfect **E**lectrical **C**onductor (PEC) boundary at $z_{min} = 0\,\mu$m. Another PEC boundary at $z_{max} = 3.15\,\mu$m, where the spherical mirror ends, is set to determine the calculation domain. The spherical mirror has a diameter of $16\,\mu$m and a radius of curvature of $80\,\mu$m. The geometry of the cavity gives its resonant frequency. The length determines the number of zeros q of the standing wave. Together with the curvature of the mirrors R and the number of zeros in radial direction m, n following resonant frequency is given [2]:

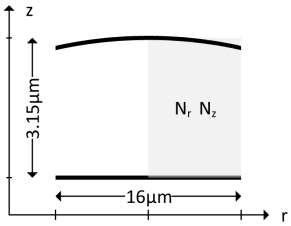

Fig. 4. 2D model of cavity

$$f_{q,m,n} = \frac{c_0}{2L}\left[(q+1) + \frac{m+n+1}{\pi} \cdot \mathrm{acos}\left(\sqrt{(1-\frac{L}{R})}\right)\right] \tag{13}$$

Equation (13) counts for equal curvature of the mirrors $R = 80\,\mu$m along the double propagation distance $L = 6.3\,\mu$mm resulting to seven axial zeros $q = 7$ and no radial or azimuthal zeros $m = n = 0$. The resonant frequency yields to $f_{7,0,0} = 193.3701653\,$THz. | FN |

1) Matlab model: Due to BOR [5] the mesh in the FIT is reduced to a 2D cutting plane with $N_r \cdot N_z$ grid points as sketched in fig. 4. Each point consists of a grid edge in r, φ and z-direction, the resulting computation domain is a so called "2.5D rz grid". The boundary at $r = 0$ is set to **P**erfect **M**agnetic **C**onductor (PMC) as symmetry condition and the boundary at $r = 8\,\mu$m is set to PEC. The spherical mirror is implemented as **P**erfect **B**oundary **A**pproximation (PBA) by adjusting the primary grid edges and primary grid facets. The PBA is represented in the equations (14) [9] by a PEC fill factor $f_{A,m}$ and $f_{L,i}$. A maximum fill factor of 95% is implemented to avoid the degradation of the system matrix condition number. The resulting primary edges are shown in fig. 5. | LS |

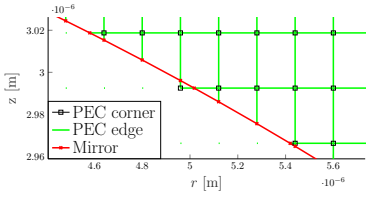

Fig. 5. Primary edges as PBA

$$(M_\mu)_{m,m} = \mu \frac{A_m}{\tilde{L}_m}(1 - f_{A,m}) \;,\; (M_\varepsilon)_{i,i} = \varepsilon \frac{\tilde{A}_i}{L_i} \frac{1}{1 - f_{L,i}} \tag{14}$$

2) CST model: The spherical mirror is defined by the "analytical face" option with a radius of $80\,\mu$m and a specified angle range (ϑ: $0-0.03188428\pi$, φ: $0-2\pi$). In radial direction the boundaries are open for the time domain calculation (fig. 8) and closed (PEC) for computing the eigenmodes. In order to excite a x-polarized electric field component, the yz-plane is set to PEC and the xz-plane to PMC which further reduces the calculation domain. | FN |

B. Numeric Solution 2.5D

The following numerical 2.5D calculations in Matlab are made with a FIT mesh consisting of $N_r \cdot N_z = 6171$ points, the average edge length is $\Delta = 0.0931\,\mu$m.

1) Time Domain: The FIT TD simulation is excited by a Gaussian shaped current (Gauss-sine in time domain and Gaussian intensity along the r axis) in the update scheme (9). The Gauss-sine for the following results is created with a frequency range of 1THz around the resonant frequency $f_{7,0,0}$ and a minimum beam radius of $2.77\,\mu$m. The excitation is added to the r directed edges in front of the plane mirror.

A **F**ield **M**onitor (FM) is implemented as described in equation (15) to extract the electric field components at the $f_{7,0,0}$ resonant frequency from a superimposed field distribution. The addition is performed at every time step, N is the total number of time steps the FM is active. In order to obtain valid results at least one signal period has to be observed.

$$\hat{\mathrm{e}}_{\mathrm{FM}} = \hat{\mathrm{e}}_{\mathrm{FM}} + N^{-1} \cdot \hat{\mathrm{e}} \cdot exp[-j2\pi f_{7,0,0} \underbrace{(n-1)\Delta t}_{\text{elapsed time}}] \qquad (15)$$

The resulting electric field component E_r of the mixed field in time domain and the FM is visualized in fig. 6 for two different simulation times. Fig. 6 (a) shows the switch-on process: the desired Gauss mode can be recognized in the field monitor but is distorted, also the superimposed field differs from the Gauss mode field distribution. Fig. 6 (b) shows the steady state condition, the Gauss mode is visible in the FM and the mixed field. The calculation time for fig. 6 (b) is about 18 minutes.

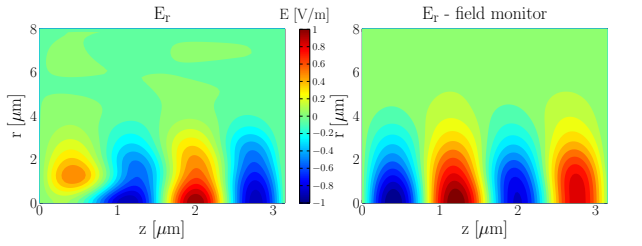

(a) Radial electric field component in the TD after $T = 0.7198$ ps (scaled to 1 V/m)

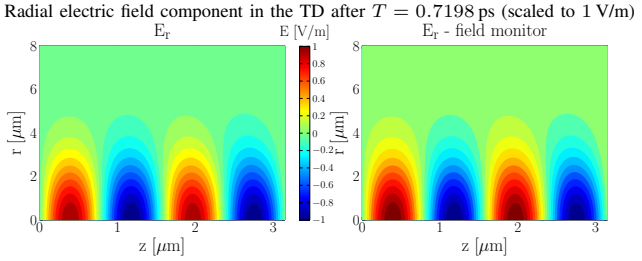

(b) Radial electric field component in the TD after $T = 25.2116$ ps (scaled to 1V/m)

Fig. 6. Electric field in the TD (scaled to 1 V/m), the field monitor shows the electric field components with the frequency $f_{7,0,0} \approx 193.37$ THz

2) Eigenmode Solver: To reduce the computational effort rows and columns with zero entries in the main diagonal of $A^{(D)}_{\mathrm{curlcurl}}$ (11) are cancelled. The deleted entries are reinserted to the calculated eigenvectors to restore the valid result dimension of the **e**igen**m**ode (EM) solution. The eigenvalues correspond to the resonant frequency $\omega^2 = (2\pi f)^2$ of the field distribution described by the eigenvector. The eigenvalue $f_{\mathrm{FIT}} \approx 193.3349$ THz is found with the smallest difference to the $f_{7,0,0}$ resonant frequency, the relevant E_r field component of the eigenvector is visualized in fig. 7 and shows the Gauss mode. The calculation time for the solution in fig. 7 is about 5 seconds in total. | LS |

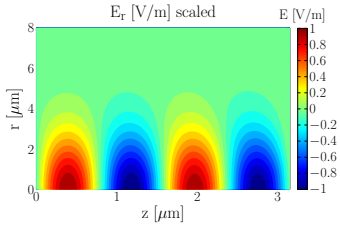

Fig. 7. Eigenmode with the resonant frequency $f \approx 193.33$ THz, scaled to 1 V/m

C. Numeric Solution 3D

The 3D solution is generated using the industry standard simulation software *CST Microwave Studio* [1] with the TD and EM solver. The excitation with a Gaussian shaped pulse shows the transient behaviour and furthermore also the steady-state condition when all field distributions except the desired one at the resonant frequency are decayed. Additionally, the finite number of modes of the closed cavity are represented by the EM solver.

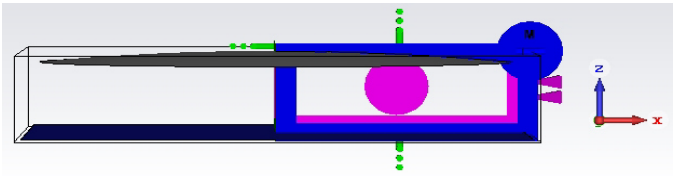

Fig. 8. CST time domain 3D model with symmetry planes and boundaries

1) Time Domain: The solver is based on FIT with hexahedral meshing offering an accurate modelling due to PBA. A macro to generate a linear polarized Gaussian beam with a power of 1W is provided in CST [1]. A bandwidth of 1 THz around the resonant frequency $f_{7,0,0}$ has been chosen. The minimum beam radius w_0 is $2.77\,\mu$m, the resolution of the source is 16 lines/λ and the truncation error is set to $\frac{1}{e^4}$. The source is placed close to the plane mirror at $z = 0.081578\,\mu$m along radial direction, as pictured in fig. 8. Different mesh resolutions have been simulated:

TABLE I
OVERVIEW OF TIME DOMAIN SIMULATION RESULTS IN CST

average edge length	**simulation period**	**PC calculation time**	**resonant frequency**
$0.09\,\mu$m	500 ps	≈ 5 h	192.8 THz
$0.06\,\mu$m	500 ps	≈ 15 h	193 THz
$0.04\,\mu$m	1000 ps	≈ 158 h	193.29 THz

The resonant frequency converges closer to the target $f_{7,0,0}$ by each mesh refinement step. Although the excitation takes only few picoseconds a much longer simulation period better approximates a steady-state condition. In order to evaluate the Gaussian shape of the fields, curves are placed in radial directions on which the field values are examined. The distance w from the z-axis determines where the fields have to be decayed by a factor of $\frac{1}{e}$, see equation (5).

2) Eigenmode Solver: The calculation of the modal field distribution and its corresponding frequency is performed using FIT and the finite element method. No losses or static modes are considered. Both mesh types as well as different

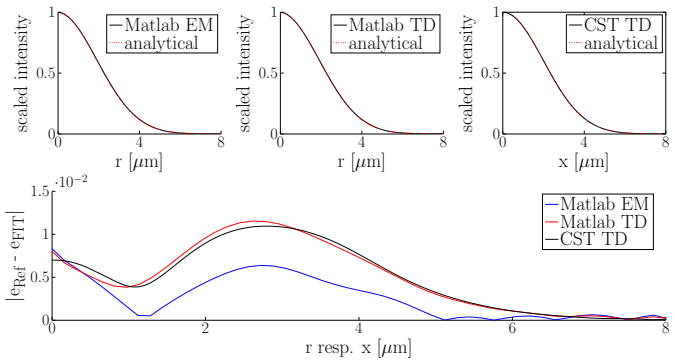

Fig. 9. Comparison of the simulated electric field values e_{FIT} with the analytical solution e_{Ref}

mesh resolutions ranging from 10 to 35 cells per wavelength are simulated. Gaussian eigenmodes are searched from 170 THz to 195 THz setting small frequency intervals within this bandwidth. However, the desired Gaussian eigenmode is not found but higher cylindrical modes dominate. | FN |

D. Evaluation

The magnitude of the radial electric field component e_{FIT} at 193.37 THz in Matlab and at 193.41 THz in CST are evaluated along radial direction at the first maximum of the mode (average edge length: $\approx 0.09\,\mu$m in Matlab, $\approx 0.04\,\mu$m in CST). The analytical solution e_{Ref} is fitted into the numerical field result e_{FIT} up to a minimal difference of $\|e_{Ref} - e_{FIT}\|$. Fig. 9 shows that the best accuracy of the results is obtained from the EM calculation in Matlab. The convergence of the simulated electric field values and the simulated resonant frequency towards the analytical solutions are examined by refining the mesh of the CST TD and the Matlab EM simulations:

$$Diff = \frac{\|e_{Ref} - e_{FIT}\|}{\|e_{Ref}\| \cdot N_r}, \quad e_{rel} = \frac{|f_{FIT} - f_{7,0,0}|}{f_{7,0,0}} \tag{16}$$

First, the convergence of the relative error $Diff$ considering e_{FIT} and e_{Ref} with regard to the number of radial mesh points N_r is shown. The relative error becomes smaller with an asymptotic error of first order, see fig. 10. Due to the long calculation times in CST (compare tab. I), only three different mesh resolutions are presented. Second, the convergence of the relative error e_{rel} considering the simulated resonant frequency f_{FIT} and the analytical solution $f_{7,0,0}$ is analysed. f_{FIT} converges to $f_{7,0,0}$ with second order as shown in fig. 11. However, at very short edge lengths the convergence flattens. This is an indication for having a different numerical resonant frequency as the analytical one. To ensure convergence a numerical reference $f_{NUM} = 193.35786$ THz has been calculated with an edge length of $0.0051\,\mu$m indicating second order convergence, as shown in fig. 11. For edge lengths close to $0.0051\,\mu$m the convergence order further increases as f_{FIT} and f_{NUM} are nearly identical. However, it is not feasible to calculate f_{NUM} for even higher mesh resolutions due to the increasing memory demand. | FN |

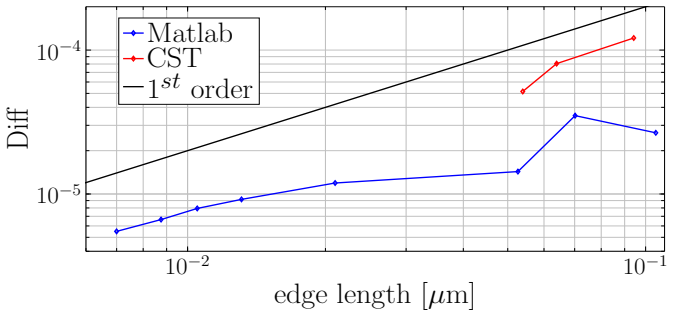

Fig. 10. Convergence of the relative error $Diff$ regarding the electric field values at different mesh resolutions

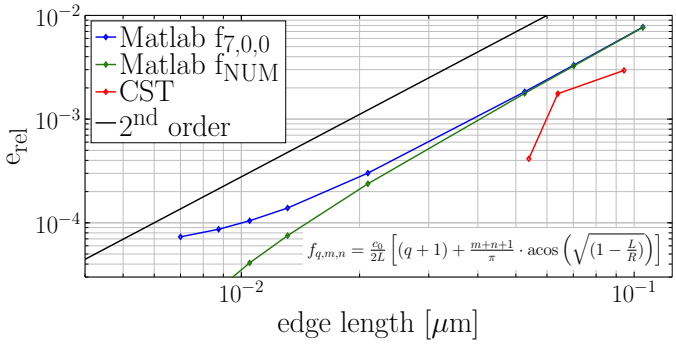

Fig. 11. Convergence of the relative error e_{rel} regarding the resonant frequency at different mesh resolutions

IV. Conclusion

This paper demonstrates numerical computations to obtain accurate field solutions for optical cavities. The presented algorithm yields the same accuracy in time domain simulation as a commercial software while calculation time can be reduced significantly. Despite easier modelling in 3D CAD software the numeric model in 2.5D offers the ability to support engineering tasks more efficiently as little calculation time makes even computer based optimization feasible. Furthermore eigenmode solutions provide an even greater accuracy as they represent a steady field solution. The search for eigenmode of higher order can be simplified in our algorithm for the desired azimuthal mode order as oppose to standard 3D implementations.| MH |

References

[1] CST, "Computer simulation technology," *microwave studio - https://www.cst.com/products/cstmws*.

[2] H. Kogelnik and T. Li, "Laser beams and resonators," *Proceedings of the IEEE*, vol. 54, no. 10, pp. 1312–1329, Oct 1966.

[3] M. Dehler, *Numerische Lösung der Maxwellschen Gleichungen auf kreiszylindrischen Gittern*, 1993.

[4] M. Clemens and T. Weiland, "discrete electromagnetism with the finite integration technique," *Progress In Electromagnetics Research*, vol. 32, no. 10, pp. 65–87, 2001.

[5] S. Kirsch, "Cylindrical and nonconformal material interfaces in the finite integration technique," 2016.

[6] K. Yee, "Numerical solution of initial boundary value problems involving maxwell's equations in isotropic media," *IEEE Transactions on Antennas and Propagation*, vol. 14, no. 3, pp. 302–307, May 1966.

[7] MATLAB, "Matrix laboratory." *https://de.mathworks.com/products/matlab.html*.

[8] R. Schuhmann, *Rotationssymmetrische Eigenwertprobleme mit PBA*, 2001.

[9] P. Thoma, *Zur numerischen Lösung der Maxwellschen Gleichungen im Zeitbereich*, 1997.